

EXTRAPOLATION OF THE STRESS INTENSITY FACTORS BASED ON DISCRETE EXPERIMENTAL RESULTS.

F. Thamm *

The stress intensity factor (SIF) is defined usually by following formulas

$$K_I = k_I \sigma_0 \sqrt{2a\pi} \quad \text{and} \quad K_{II} = k_{II} \tau_0 \sqrt{2a\pi}$$

for fracture-modes I and II respectively, with the full or half crack-length a , the "far-field" stress σ_0 or τ_0 , and a dimensionless quantity k depending on the boundary conditions. It is shown, that the actual influence of a upon the SIF is diminishing with its growing value and in many cases the SIF depends practically on the far-field stress only. This makes an extrapolation method possible which is checked by two photoelastic experiments.

In linear elastic fracture mechanics the stability of a crack is governed by the stress intensity factor (SIF) [1][2]. It is based on the Westergaard stress function with complex variables, which is derived for the case of a crack with the length $2a$ in an infinite plate loaded perpendicularly to the plane of crack. In case of the traction in the y -direction this can be written as follows [3]

$$Z = \sigma_0 \frac{z}{\sqrt{z^2 - a^2}} \quad (1)$$

with the complex variable $z = x + iy$ and the far-field stress σ_0

The development of the stress components σ_x , σ_y and τ_{xy} as a function of x and y leads to complicated expressions [4] and therefore the practice restricts itself to obtain approximations for the region around the crack-tip. These well-known equations contain the SIF in the following form (for fracture-mode I):

$$K = K_I = \sigma_0 \sqrt{2a\pi} \quad (2)$$

* Department of Mechanical Engineering
Technical University of Budapest.

For other shapes of the cracked specimen the SIF-s can be obtained theoretically or experimentally and are usually written for the fracture-modes I and II in the following form:

$$K_I = k_I \sigma_0 \sqrt{2a\pi} ; K_{II} = k_{II} \tau_0 \sqrt{2a\pi} \quad (3)$$

with σ_0 and τ_0 the far-field stresses and a a characteristic crack-length.

Eqs. (3) can create the impression of a tight dependence between the SIF and the crack length. But as k_I and k_{II} also depend on the crack-length, actually in many cases $k_I \sqrt{a}$ and $k_{II} \sqrt{a}$ can be more or less independent from a . In fact the formulas for the stress distribution can be derived also from the stress-function [5]:

$$Z = \frac{K}{\sqrt{2\pi z}} \quad (4)$$

in which the crack-length a does not appear and K only depends from the boundary conditions. If the crack-length can be considered as "infinite" against the region in which the stress distribution described by (4) assumed to be valid, K is only dependent from σ_0 or τ_0 respectively. If the SIF belonging to a far-field stress σ_{01} or τ_{01} is obtained by some experimental or numerical method, the equivalent value for different boundary conditions including different crack-lengths denoted by the subscript 2 can be written

$$K_{I2} = \frac{\sigma_{02}}{\sigma_{01}} K_{I1} \text{ and } K_{II2} = K_{II1} \frac{\tau_{02}}{\tau_{01}} \quad (5)$$

The estimation expressed by eqs. (5) seems to be very rough and should be restricted to "similar" cases, when only the crack length varies leaving all other boundaries of the specimen unchanged. Even in this case doubts may arise about their justification and therefore twodimensional photoelastic experiments were carried out for their verification.

Isochromatic fringe patterns were taken from the models with different crack-lengths and the SIF-s were evaluated by the tangent method described by Ruiz [6] for fracture mode I (Fig 1.) K_I is then obtained from the slope of the distribution of $\sigma_1 - \sigma_2$ along the y -axis plotted over $1/\sqrt{2\pi y}$. As shown by Schroedel and Smith [7] for small values of σ_{x0} the plot is practically linear and thus enables the additional evaluation of σ_{x0} .

For the evaluation of K_{II} the method of Smith et al [8] was used as shown in Fig.2. The distribution of $(\sigma_1 - \sigma_2)^2 \cdot 2\pi x$ along the x -axis was plotted over $2\pi x$. The value of the curve at point $x = 0$ yielded K_{II}^2 .

The specimen used for the determination of K_I is shown in Fig.3. The crack was initiated at point A and a series of static experiments with different crack-lengths along line AC were carried out. Two of the fringe patterns are shown in Figs.4. and 5. The experiment with crack-length $a=40$ mm was taken as the basis of the extrapolation. The far-field stress was calculated elementary for traction and bending with the notations of Fig.3.

$$\sigma_0 = \frac{F}{v(h-a)} \left[1 + \frac{3(h+2a)}{2(h-a)} \right] \quad (6)$$

Fig.6. shows the measured SIF-s(full line) and the extrapolated values (dotted line). As seen from the figure, the agreement between the measured and the extrapolated values was very satisfactory for the region $a = 10-50$ mm.

The specimen for the K_{II} -determination is shown in Fig.7. The cracks were produced from both sides along line AB symmetrically. A series of fringe patterns is shown in Fig.8. As the evaluation of the far-field stress is somewhat uncertain in this case, an evenly distributed shear stress along the cross section between the crack-tips was taken into account a far-field stress by the formula

$$\tau_0 = \frac{F}{v(m-2a)} \quad (7)$$

The measured values of K_{II} are plotted against the crack-length in Fig.9. and are drawn with full line. The extrapolation based on the measured point at $a=7,5$ mm is shown by a dotted line. The agreement between measured and extrapolated data is much worse than in the previous experiment which may be connected with the uncertainty of the assumption of the far-field stress as mentioned above. Nevertheless the trend of the measured and the extrapolated curve is similar which gives some hope for a better extrapolation approach perhaps like the analogy introduced by Herrmann [9]. It is desired to continue these investigations to get more detailed knowledge about the applicability of the extrapolation method described.

REFERENCES

- [1] Griffith, A.A.: The Phenomenon of Rupture and Flow of Solids. Phil. Trans. Roy. Soc. London. A. 1920.
- [2] Paris, P.C.-Sih, G.C.M.: Stress Analysis of cracks. Fracture Toughness Testing and its Applications. ASTM Publication No. 381. 1965.
- [3] Westergaard, H.M.: Bearing Pressures and Cracks. Journal of Applied Mechanics. 1939. pp. A-40 - A-53.

- [4] Szabó, V.: Stav napätia v okolí šikmej trhliny pri drojosovom namchání. Stavebnicky Časopis 31(1983) Nr.3.
- [5] Rossmanith, H.P.: Analysis of Mixed-Mode Isochromatic Crack-Tip Fringe Patterns. Acta Mechanika 34(1979) pp.1-38.
- [6] Ruiz, C.: Experimental Determination of Stress Distribution around Notches and Slits in Cylindrical Pressure Vessels. Proc.4.Int.Conf. on Exp.Stress Analysis. Cambridge. Inst. of Mech,Engineers.1970. pp.363-371.
- [7] Schroedl, M.A.-Smith, C.W.: Local Stress Near Deep Surface Flaws Under Cylindrical Bending Fields. Progress in Flaw Growth and Fracture Toughness Testing. ASTM STP 536. ATM(1973) pp.45-63.
- [8] Smith, C.W.-Jolles, M.-Peters, W.H.: Stress Intensities for Nozzle Cracks in Reactor Vessels. Exp.Mech. XXXIV/2(1977) pp.449-454.
- [9] Herrmann, G.: Mechanics in Material Space with Applications to Defects and Fractures in Elastic Solids. Lecture held at the Hungarian Academy of Science. 1988 .

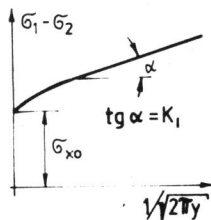
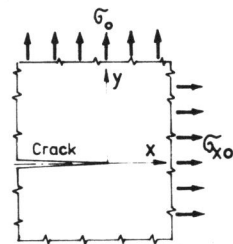


Fig. 1 The tangent method for evaluating of SIF K_I from the photoelastic isochromatic fringe pattern as the slope of the distribution of $(\sigma_1 - \sigma_2)$ over $1/\sqrt{2\pi y}$

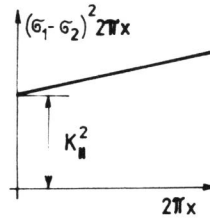
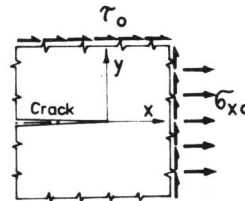


Fig. 2 The method of evaluation of the SIF K_{II} from the isochromatic fringe pattern, extrapolating the distribution $(\sigma_1 - \sigma_2)^2 2\pi x$ to $x = 0$

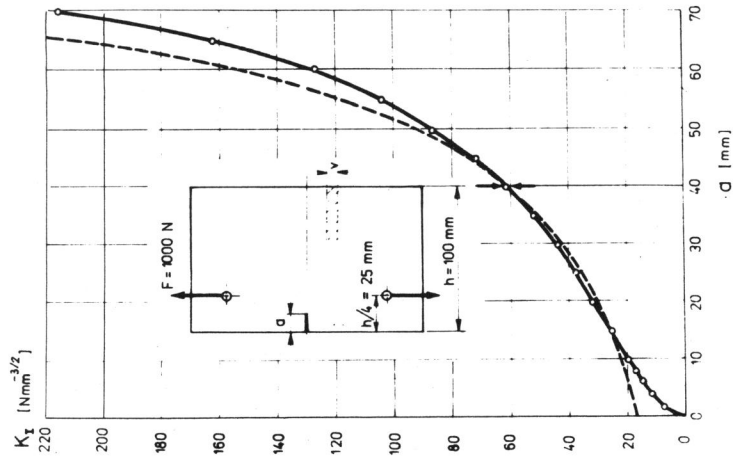


Fig. 6 The SIF K_I plotted over the crack depth a . Full line: measured values from the fringe patterns. Dotted line: calculated from formulas (5) and (6) from the value at $a = 40$ mm.

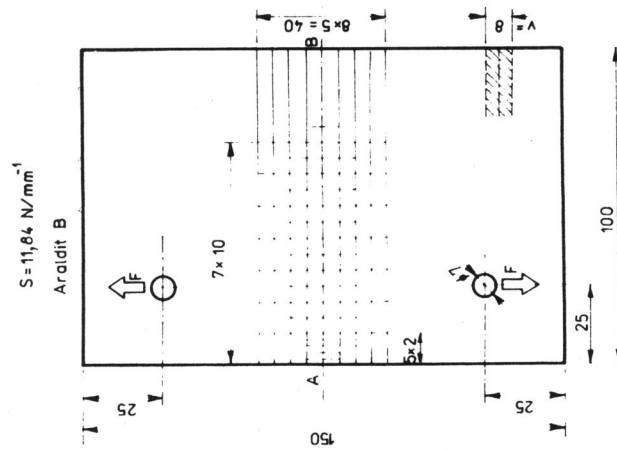


Fig. 3 The specimen for the determination of K_I . The crack has been produced in 18 steps along line AB beginning at point A.

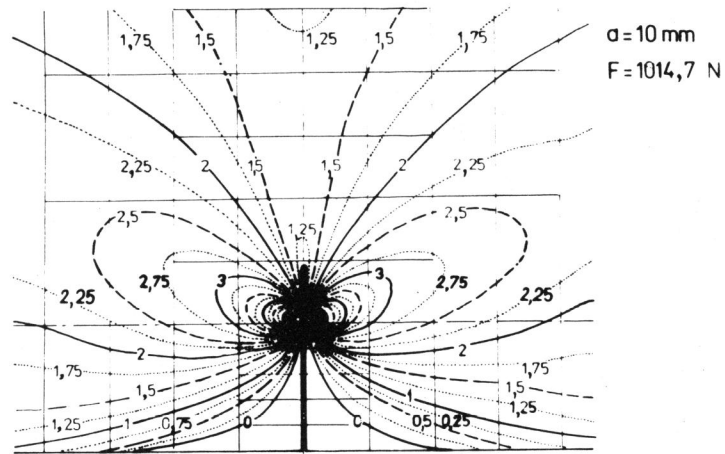


Fig. 4 Isochromatic fringe pattern of the specimen in Fig.3. for a crack-length of $a = 10$ mm

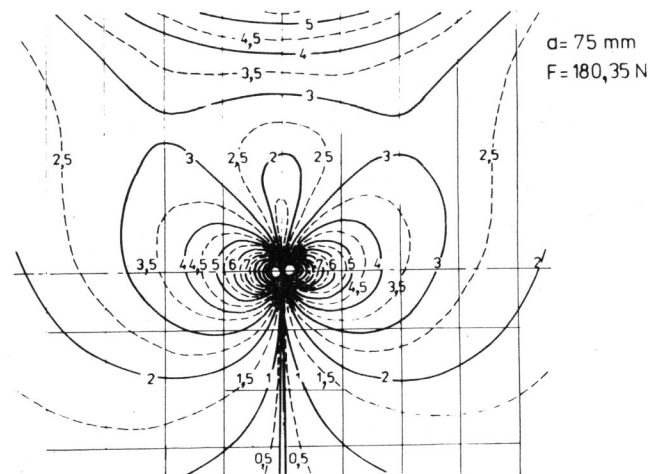


Fig. 5 Isochromatic fringe pattern of the specimen in Fig.3. for a crack-length of $a = 75$ mm.

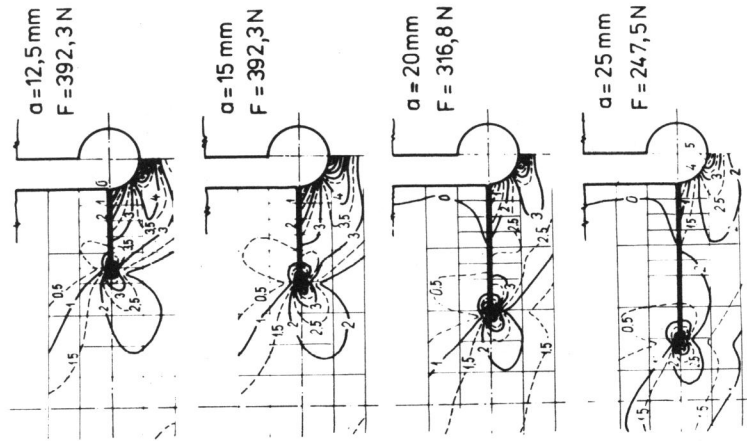


Fig. 8 A series of fringe-patterns taken from the model of Fig.7. for different crack-depths.

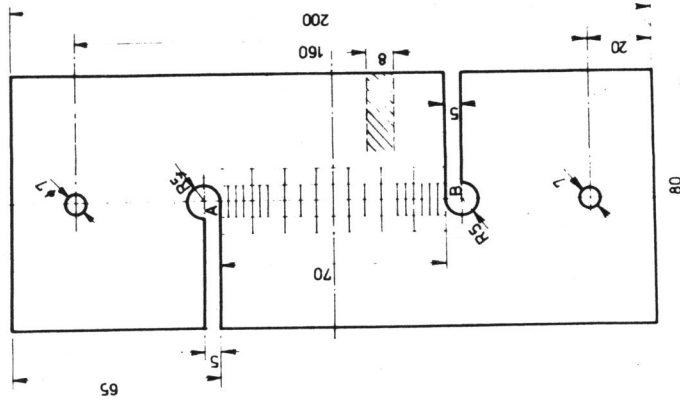


Fig. 7 the specimen for the determination of K_{II} . The cracks starting at both ends of the line AB were produced in 10 steps of the crack-length.

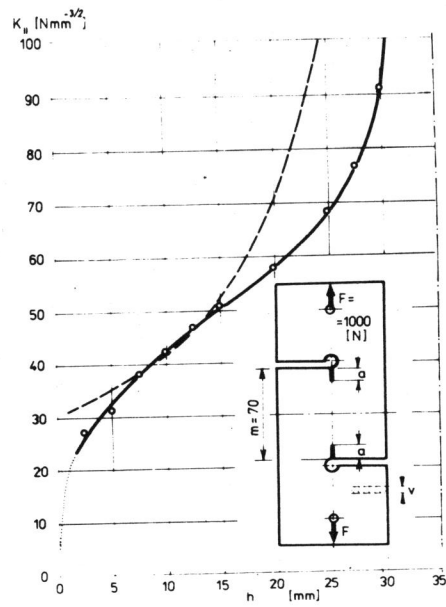


Fig. 9 The SIF K_{II} plotted over the crack-depth a .
 Full line: measured values
 Dotted line: Calculated from formulas (5) and (7) based on the measured value at $a = 7,5$ mm.